

FLOW ESTIMATION USING NEURAL NETWORKS

Li Vodinh Lorang, Bérengère Podvin, Patrick Le Quéré

Departement of Mechanic and Energetics,
LIMSI-CNRS

BP 133, 91430 Orsay Cedex, France
li.vodinh@limsi.fr, berengere.podvin@limsi.fr, plq@limsi.fr

ABSTRACT

Neural networks have been used with some success for turbulence control and in particular drag reduction on a flat wall. Here we examine how results from the POD analysis of an uncontrolled channel flow can be combined into a neural-based strategy for drag reduction. Numerical experiments are performed in a flat channel of relatively small horizontal dimensions, so that the flow there is relatively simplified.

INTRODUCTION

Over the past few years the control of turbulence has been the object of a substantial effort. Several reviews of flow control techniques can be found in Gad-el-Hak [1], Lumley and Blossey [2] or Bewley [3]. Results from optimal control theory have been applied to the equations of Fluid mechanics, in particular by Bewley *et al.* [4], and Choi *et al.* [5]. More recently, state estimators for the linearized Navier-Stokes equations have been developed [6] to account for the lack of information available about the flow in practice.

Another approach relies on low-dimensional modelling. An appealing technique for this purpose is the POD (see for instance [7]), which extracts the most energetic structures of the flow. However, the controlled flow may not lie anymore on the subspace spanned by the uncontrolled eigenfunctions [8], although it seems likely that the vortical structures exhibited by the POD decomposition are essential to the turbulence generation mechanism and should still bear some relation to the controlled flow [9]. Realistic modelling should therefore adapt itself to the modifications brought to the flow, which is not easy to achieve.

A more empirical approach to control is based on experiments, most often performed numerically. One very popular strategy is the opposition control strategy by Choi, Moin and Kim [10], which has been the starting point for a number of investigations. These include the development of neural networks to estimate the actuation needed from available measurements of the flow. Neural-based experiments have been performed both in the laboratory (Reynolds and Jacobson [11]) and numerically (Lee *et al* [12]).

In this paper we try to combine insights from the POD description into a neural networks approach. The POD approach can be viewed as a particular type of neural networks (see Koumoutsakos 2002 [13]). However, a potential pitfall to take into account is that the POD gives a global description of the flow - every structure extends over the whole physical domain - whereas a control strategy should be localized in the physical space.

The paper is organized as follows: following the approach of Lee *et al.* [12], we first implemented a neural network algo-

rithm to predict the velocity field from transverse wall shear measurements. Next, we showed that these measurements were well correlated with the projection of the full velocity field on some characteristic structure (the dominant POD structure of the uncontrolled flow) that we consider essential to the turbulence-generating process. We then developed a neural-based algorithm to estimate this POD structure from wall shear stress measurements.

NEURAL NETWORK'S MAIN FEATURES

We first built a neural network similar to the one described by Lee *et al.* [12]. This neural network aims to find a correlation between wall-shear stress and wall actuations from given data sets. We only use the transverse wall-shear stress $\frac{\partial w}{\partial y}$ as the adding of $\frac{\partial u}{\partial y}$ was not relevant for the neural network performance. The desired wall actuations is the one recommended by Choi *et al.*[10] i.e. the opposite of the velocity at $y^+ = 10$. This strategy of blowing and suction at the wall brings about a drag reduction of 25% by reducing the sweep and ejection events in the wall-layer. The advantage of using neural network compared to other control strategies is that it is able to predict the wall actuations directly from the wall shear stress which is easily measurable in real applications.

Description of the neural network

It is a standard two-layer feedforward network with hyperbolic tangent hidden units and a linear output unit. It was shown that it was possible to evaluate the wall actuation in one point using only the values of wall shear stress in the spanwise direction. So the function describing the neural network output is:

$$v_{jk}^{net} = W_a \tanh \left(\sum_{i=-(N-1)/2}^{(N-1)/2} W_i \frac{\partial w}{\partial y} \Big|_{j,k+i} - W_b \right) - W_c \quad (1)$$

with $1 \leq j \leq N_x$ and $1 \leq k \leq N_z$

N is the number of neighboring points in the spanwise direction. N_x and N_z are respectively the number of gridpoints in the streamwise direction and in the spanwise direction. The W 's are the weights of the neural network that are established during a learning process. This learning process is based on a simplex algorithm used to train the neural network obtaining the desired Choi actuation by minimising the error defined in

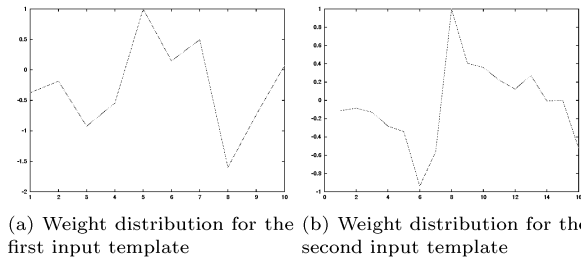


Figure 1: Weight distributions for the two inputs template

(2), where v_{jk}^{des} represents sets of Choi's wall velocity field.

$$error = \frac{1}{2} \sum_j \sum_k e^{\lambda |v_{jk}^{des}|} (v_{jk}^{des} - v_{jk}^{net})^2 \quad (2)$$

Learning process and off-line control

The training data consist of several samples of 2D fields of velocity at $y^+ = 10$ and wall shear stress at different time. Those data sets were carried out with a 3D direct numerical simulation of a fully turbulent channel flow. The numerical procedure based on a pseudo-spectral solver is the one described by Kim et al [14], that has shown to be popular in this area. The size of the computational box has been chosen to include in its width two pairs of low/high-speed streaks on statistical average. We used then a computational domain $(Lx, Ly, Lz) = (4\pi/3, 2, 4\pi/3)h$, and a grid resolution of (96,65,48). The Reynolds number based on the channel half-height h and center line velocity is 4000 and the one based on h and friction velocity u_* is about 140. This configuration is less complex than a fully turbulent flow but ensures that the essential dynamics are retained, see Podvin for more details [15].

Regarding the neural network architecture, we tried two types of input templates: one with 7 neighboring points and the other one with 13 neighboring points corresponding respectively to 70 wall units and 130 wall units in the spanwise direction (Fig.1). The weights in the first case did not converge while those in the second case showed good convergence already with 20 samples. It seems that with 7 neighboring points the input template is not large enough to capture all the informations from the flow that influences that point. The input template must encompass the size of one coherent structure, which is about 100 units wide. In the second case the error reached its asymptotic limit within 100 training periods. To test the validity of the converged weights we put as boundary condition the velocity at the wall given by the neural networks.

By implementing the new boundary conditions at the bottom wall in the channel flow simulation, we obtained 20% drag reduction (Fig.2) which is the reduction obtained by Lee et al. The visualisation of the resulting flow shows us that as regards streamwise vorticity the mean flow remains unchanged unlike the near-wall structures which have less intensity (Fig.3).

LINK BETWEEN THE SHEAR AND THE MAIN FLOW DYNAMICS

The performance of the neural network described above let us think that there is a strong link between the wall shear

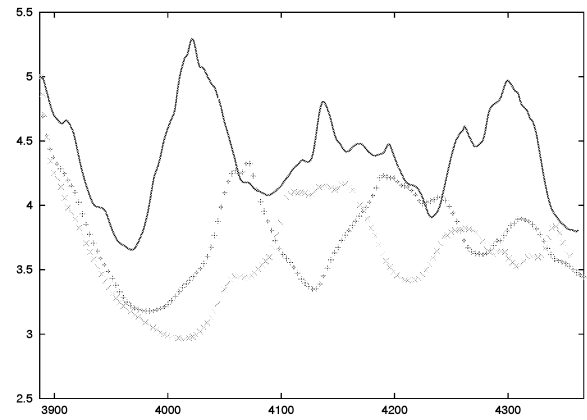


Figure 2: Spatially averaged drag histories with three types of boundary conditions: – no control x Choi + neural network

stress and the velocity at $y^+ = 10$ where the turbulence production is the most important. To bring to the fore this phenomena we used Proper Orthogonal Decomposition that is able to extract the main features of the flow. POD is an appropriate tool in the study of channel flow owing to the presence of coherent structures in the wall-layer. In our case the first structure and the three first three structures, respectively account for 60% and 90% of the total kinetic energy of the wall region [16].

POD splits up the velocity fields into time-depending coefficients and a space-depending basis so that the velocity fluctuations can be written as:

$$\mathbf{u}(x, y, z, t) = \sum_{n=1}^{\infty} a^n(t) \psi^n(x, y, z) \quad (3)$$

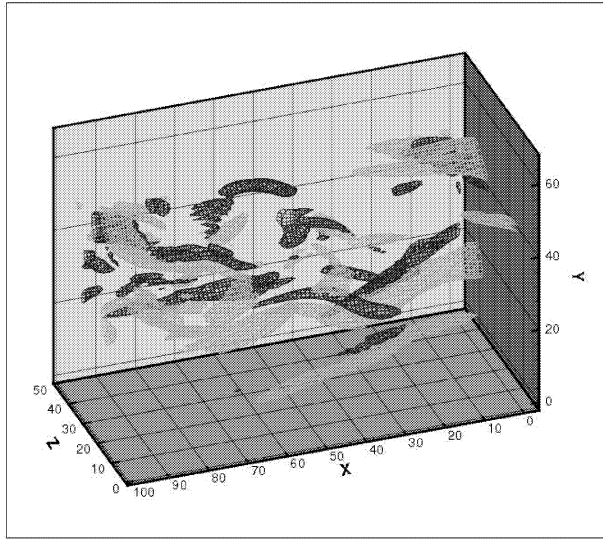
The decomposition is optimal in the sense that the first n POD eigenfunctions capture more energy than any other decomposing set of n elements. So the first eigenfunction conveys the most important mechanism of turbulence generation as it represents the most energetic structure of the flow. The computational box is periodic in x and z so that the POD eigenfunctions in those directions are simply Fourier modes. It is more practical in this case to work in Fourier space. In this space, the velocity fluctuations are defined by:

$$\hat{\mathbf{u}}_{kx,kz}(y, t) = \sum_{n=1}^{\infty} a_{kx,kz}^n(t) \psi_{kx,kz}^n(y) \quad (4)$$

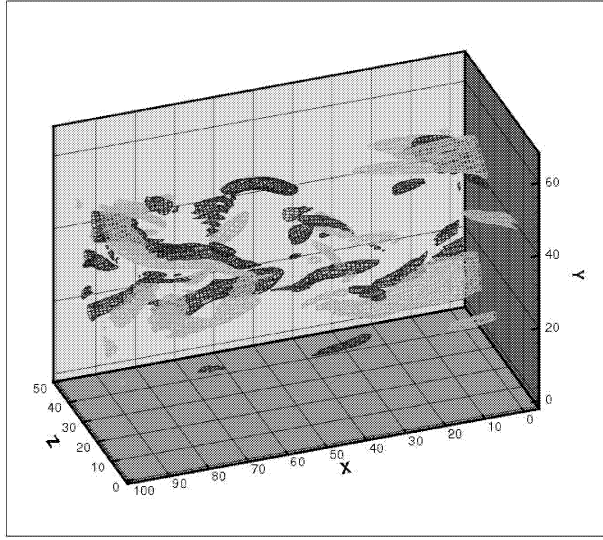
As we project the velocity field on the first eigenfunction ($n = 1$), we observe the correlation between the extracted velocity and wall shear stress. Let us call \hat{v} the projection of normal velocity onto the first eigenfunction of the uncontrolled flow. The resulting curves (Fig.4a and 4b) revealed that \hat{v}^* and $\frac{\partial \hat{u}}{\partial y}$ were well correlated in the uncontrolled flow. The relation can be written as:

$$\hat{v}^* \simeq iC \frac{\partial \hat{u}}{\partial y} |_{y=0} \quad (5)$$

This control law is very similar to the one suggested by Lee et al, but this time we consider the projection of the velocity field on the first mode. C was found to be about 10 outer units. As we controlled the flow with Choi's actuation and projected the resulting normal velocity on the same uncontrolled eigenmode, the wall shear and the projection of the velocity field



(a) simulation with no control



(b) simulation controlled at the wall by the neural network

Figure 3: Streamwise vortex isosurface in the channel with two opposite intensity, darker structures 0.04 and lighter structures -0.04

remain well correlated (see Fig. 4c and 4d). This suggests that even though POD eigenfunctions are modified when control is applied, uncontrolled POD eigenfunctions are still relevant to describe some of the flow dynamics. The wall-shear stress is then a good indicator of drag reduction as his time-evolution is directly linked with the behaviour of the most energetic structure that develop itself in all the flow.

POD AND NEURAL NETWORK

In this part, we use a neural network approach to better model the relationship - approximated as a linear one in the previous section - between the wall shear stress and the POD eigenmode. This neural network is built to estimate the three first complex time-varying eigenmodes of the first POD mode, i.e. a_{01}^1 , a_{02}^1 and a_{03}^1 directly from the wall-shear measurements. Aid of eigenmode and wall-shear data sets extracted

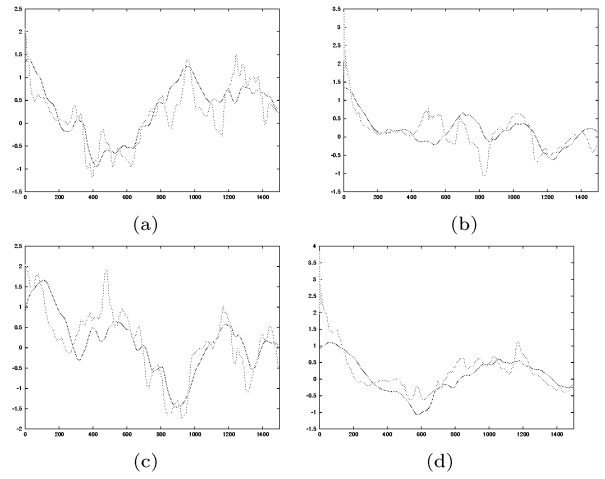


Figure 4: Time evolution of the projection of the velocity field on the first POD mode v_{01}^* - and the rescaled wall shear $i \frac{\partial \hat{w}_{01}}{\partial y}$ -, a)b)controlled flow, c)d)uncontrolled flow, a)c)real part, b)d)imaginary part

from the uncontrolled flow, we tried to correlate those data using the same type of neural network as in the first section.

$$Re(a_{0k}) = W_a \tanh \left(\sum_{k=1}^3 W_i \frac{\partial Re(\hat{w}_{0k})}{\partial y} + W_{i+3} \frac{\partial Im(\hat{w}_{0k})}{\partial y} - W_b \right) - W_c \quad (6)$$

$$Im(a_{0k}) = W_a \tanh \left(\sum_{k=1}^3 W_i \frac{\partial Re(\hat{w}_{0k})}{\partial y} + W_{i+3} \frac{\partial Im(\hat{w}_{0k})}{\partial y} - W_b \right) - W_c \quad (7)$$

The learning process reached good convergence with 500 samples, and the resulting a^{net} was more effective than a the simple linear law given by the suboptimal control (see. table 1).

Table 1: Correlation rate between wall shear stress and v

v mode	suboptimal control	neural network
mode(0,1) real part	0.78	0.85
mode(0,2) real part	0.80	0.91
mode(0,3) real part	0.67	0.79
mode(0,1) imaginary part	0.83	0.87
mode(0,2) imaginary part	0.78	0.87
mode(0,3) imaginary part	0.55	0.66

By implementing the new boundary condition for the wall-normal velocity $v_{kx,kz}^{control}(0) = -a^{net} \psi_{kx,kz}^1(10)$ in the 3D simulation we obtained a substantial drag reduction (20%) (Fig.6). This strategy is quite appealing as it brings out the potential of using wall-shear measurements for drag reduction.

CONCLUSION

In this work we tried to enhance the link between turbulence production mechanism and wall shear measurements

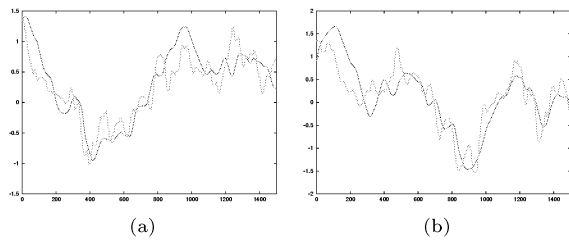


Figure 5: Time evolution of the projection of the velocity field on the first POD mode v_{01}^* – and the rescaled wall shear $i \frac{\partial \hat{w}_{01}}{\partial y}$ – a) controlled flow, b) uncontrolled flow, a) c) real part, b) d) imaginary part

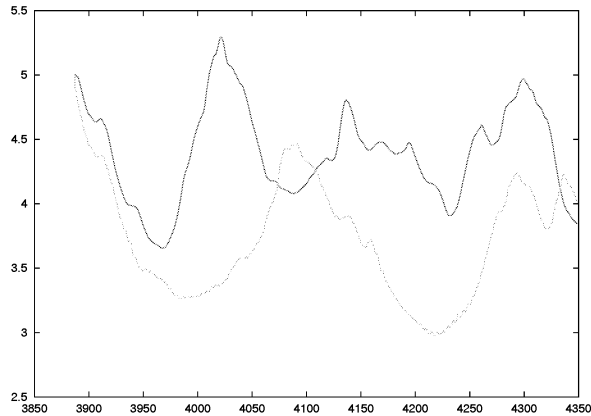


Figure 6: Spatially averaged drag histories with: – no control – - neural network

by the means of two approaches: Neural networks and POD analysis. By combining the two approaches, we hope to develop new strategies for drag minimization using realistic wall measurements.

*

References

[1] Gad-el-Hak, M., “Modern developments in flow control,” *Applied Mechanics Review*, Vol. 49, No. 7, 1996, pp. 365–379.

[2] Lumley, J. L. and Blossey, P. N., “Control of turbulence,” *Annual Review of Fluid Mechanics*, Vol. 30, 1998, pp. 311–327.

[3] Bewley, T. R., “Flow control: new challenges for a new Renaissance,” *Progress in Aerospace Sciences*, Vol. 37, 2001, pp. 21–58.

[4] Bewley, T. R. and Moin, P., “Optimal control of turbulent channel flows,” *Active control of vibration and noise*, Vol. 75, ASME DE, 1994, pp. 221–227.

[5] Choi, H., Temam, R., Moin, P., and Kim, J., “Feedback control for unsteady flow and its application for the stochastic burgers equation,” *Journal of Fluid Mechanics*, Vol. 253, 1993, pp. 509–543.

[6] Hogberg, Bewley, T. R., and Henningson, D. S., “Linear feedback control and estimation of transition in plane

channel flow,” *Journal of Fluid Mechanics*, Vol. 481, 2003, pp. 149–175.

[7] Holmes, P., Lumley, J. L., and Berkooz, G., “turbulence, Coherent Structures, Dynamical systems and Symmetry,” *Cambridge University Press*, 1996.

[8] Collis, S. S., Chang, Y., Kellog, S., and Prabhu, R. D., “Large eddy simulation and turbulence control,” *AIAA Paper 200-2564*, 2000.

[9] Podvin, B., “A P.O.D.-enhanced strategy for drag reduction in the wall-layer,” *unpublished*.

[10] Choi, H., Moin, P., and Kim, J., “Active turbulence control for drag reduction in wall-bounded flows,” *Journal of Fluid Mechanics*, Vol. 262, 1994, pp. 75–110.

[11] Jacobson, S. A. and Reynolds, W. C., “An experimental investigation towards th active control of turbulent boundary layers,” Tech. rep., Stanford University, 1995, Department of Mechanical Engineering Report No.TF-64.

[12] Lee, C., Kim, J., Babcock, D., and Goodman, R., “Application of neural networks to turbulence control for drag reduction,” *Physics of Fluids*, Vol. 9, No. 6, June 1997, pp. 1740–1747.

[13] Milano, M. and Koumoutsakos, P., “Neural network modeling for near wall turbulent flow,” *Journal of Computational Physics*, Vol. 182, 2002, pp. 1–26.

[14] Kim, J., Moin, P., and Moser, R., “Turbulence statistics in fully developed channel flow at low Reynolds number,” *J. of Fluid Mech.*, Vol. 177, 1987, pp. 133–166.

[15] Podvin, B., “On the adequacy of the ten-dimensional model for the wall layer,” *Physics of fluids*, Vol. 13, 2001, pp. 210–224.

[16] Aubry, N., Holmes, P., Lumley, J., and Stone, E., “The dynamics of coherent structures in the wall region of the wall boundary layer,” *Journal of Fluid Mechanics*, Vol. 192, 1988.